A design study of a magnifying magnetic lens for proton radiography*

YANG Guo-Jun(杨国君)[1)] ZHANG Zhuo(张卓) WEI Tao(魏涛) HE Xiao-Zhong(何小中)
LONG Ji-Dong(龙继东) SHI Jin-Shui(石金水) ZHANG Kai-Zhi(张开志)

Institute of Fluid Physics, CAEP, Mianyang 621900, China

Abstract: Magnifying magnetic lenses can be used in high-energy proton microscopes. The $-I$ lens suggested by Zumbro is analyzed in this paper, and a new type of magnetic lens called a lengthened lens is introduced. Theoretical analysis shows that the lengthened lens can form a magnifying lens, and at the same time the main advantages of a Zumbro lens are inherited. Using the My-BOC beam dynamics code, an example of the design is shown. The results show that the method of designing magnifying magnetic lenses is effective.

Key words: magnetic lens, magnifying, proton radiography, My-BOC code

PACS: 29.20.-c **DOI:** 10.1088/1674-1137/36/3/010

1 Introduction

High-energy proton radiography is a powerful tool for the diagnosis of dense objects [1, 2]. Since the transmitted protons undergo multiple coulomb scattering (MCS), the image may be seriously blurred. A magnetic lens is used to cancel the effects of MCS. Zumbro, Mottershead and Morris suggested a type of lens whose first-order transfer matrix is the $-I$ matrix [3]. The major part of the chromatic aberration is canceled by the lens, which is very useful for proton radiography. However, the magnification is confined to −1. In proton microscope systems, magnifying lenses must be used. In this paper, the design method of a magnifying magnetic lens is studied.

2 Description of the $-I$ lens [3, 4]

Generally, the first-order transfer matrix R of an imaging lens maps a particle with initial coordinates $(x,\ \theta)$ to a final position $x_{\rm f}=R_{11}x+R_{12}\theta$. Point-to-point imaging means$R_{12}=R_{34}=0$, so the final position is independent of the initial angle.

A quadrupole beamline is reflection symmetric if its second half is a mirror image of the first half. The configuration +A−B+B−A is an example of this. The symmetry forces the following relationships:

$$\begin{aligned} R_{34}&=R_{12},\quad R_{43}=R_{21},\\ R_{33}&=R_{22},\quad R_{44}=R_{11}. \end{aligned} \tag{1}$$

The magnetic lens suggested by Zumbro has four uniform quadrupoles, which form two uniform doublets. The drift spaces at the front and end of each doublet have the same length. This type of lens is called a Zumbro lens, and is shown Fig. 1. Here, k is the strength of the quadrupoles, l is the length of the quadrupoles, and D_1 and D_2 are the lengths of the drift spaces.

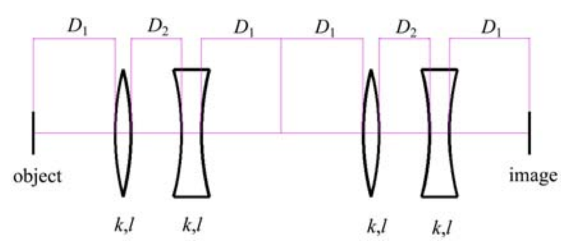

Fig. 1. A Zumbro lens.

In a Zumbro lens, each doublelet and the total lens are all reflection symmetric.

If the first-order transfer matrix of each doublet is H, the transfer matrix of the magnetic lens can be

Received 16 May 2011
* Supported by Foundation of Chinese Academy of Engineering Physics
1) E-mail: baita00@yahoo.com.cn

shown as the following:

$$R = H^2 = -I\det(H) + H \cdot \mathrm{tr}(H). \tag{2}$$

If $\mathrm{tr}(H) = 0$, the transfer matrix is $-I$ and the point-to-point conditions are satisfied.

If the injected beam is dispersive, the chromatic matching condition should be satisfied,

$$R'_{11} + \omega R'_{12} = 0, \tag{3}$$

here prime denotes the differential to momentary dispersion. The injected beam is regarded as emitting from a virtual point, so $\theta = \omega x$, and ω is the coefficient. As emittance exists, the actual relationship should be $\theta = \omega x + \varphi$.

When the injected beam is matched, the position error of a particle is written as follows:

$$B = C\varphi\Delta, \tag{4}$$

here φ is the angle dispersion, Δ is the momentary dispersion, and $C = R'_{12}$ is called the chromatic factor. C can be written as T_{126} in the transport notation.

Angle sorting is a very important function for magnetic lenses, since it can be used to distinguish materials. The Fourier plane has an angle sorting function, which means that the position of a particle at this plane is determined by its initial angle only, and is independent of its initial position.

For a Zumbro lens, the Fourier planes of both the x- and y-planes are at the middle of the lens,

$$x_{\mathrm{mid}} = H_{12}\varphi. \tag{5}$$

There are many advantages of Zumbro lenses. For example, point-to-point imaging, equal magnification ($R_{11} = R_{33} = -1$), coincided Fourier planes, simple operation (the same excitation for all quadrupoles), and so on.

3 Analysis of the magnifying lens

Like the $-I$ lens, when we have enough quadrupoles there are infinite modes for us to get a magnifying lens.

The main design constraints are imaging ($R_{12} = R_{34} = 0$) and equal magnification ($R_{11} = \pm R_{33}$) in both planes.

We expect to retain the main features of the $-I$ lens.

The reflection symmetric feature of the $-I$ lens makes the configuration very simple. But this feature cannot be retained, otherwise we will get $R_{11} = 1/R_{33}$ since Eq. (1).

The nearest way to retain this feature is to add a drift space after the reflection symmetric structure. We call this structure the lengthened lens, and it is shown in Fig. 2. Here, k_1, k_2, l, D_1 and D_2 are similar to Fig. 1, f_1 and f_2 are the focus length of the quadrupoles with a thin lens approximation, and d is the length of the added drift space.

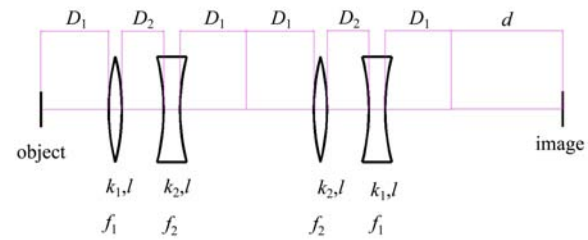

Fig. 2. The configuration of the lengthened lens.

We write the transfer matrix of the reflection symmetric structure as $R0$, and the total transfer matrix as R. Since Eq. (1), we can write $R0$ as follows:

$$R0_x = \begin{bmatrix} R0_{11} & R0_{12} \\ R0_{21} & R0_{22} \end{bmatrix}, \tag{6}$$

$$R0_y = \begin{bmatrix} R0_{22} & R0_{12} \\ R0_{21} & R0_{11} \end{bmatrix}. \tag{7}$$

Point-to-point imaging forces $R_{12} = R_{34} = 0$, which gives the following condition:

$$R0_{11} = R0_{22}. \tag{8}$$

When condition (8) is satisfied, we can get the magnification M, and the length of the drift space d,

$$M_x = M_y = 1/R0_{11}, \tag{9}$$

$$d = -R0_{12}/R0_{11}. \tag{10}$$

A thin lens approximation is then used to get further results.

From Eq. (8), the imaging condition can be written as follows:

$$D_1(D_2^2 + (f_1 - f_2)f_2) = D_2 f_2^2. \tag{11}$$

The magnification can be written as:

$$M = \frac{T}{-T + S}. \tag{12}$$

Here, $T = f_1(D_2^2 + (f_1 - f_2)f_2)^2$ and $S = 2(f_1 - f_2)^2 f_2(D_2^2 + f_1 f_2)$. In the above expressions, T is positive and S is not negative.

When $f_1 = f_2$, we see that M_x and M_y are both -1, and the length of drift space d is zero. We now get the Zumbro lens.

When f_2 deviates from f_1, S is growing from zero to positive infinity. Now we know that when S is close to T, we can get an arbitrary magnification.

The dispersion of the beam should also be considered. The injected beam is regarded as emitting from a virtual point. From the particle coordinate map we get the matching condition $R'_{11}+\omega R'_{12}=0$, which has already been shown in Eq. (3).

When the injected beam is matched, the particle position at the image plane can be written as $x_f = R_{11}x_0 + R'_{12}\varphi\Delta$ [5]. The position error in the object coordinates can be written as follows:

$$B=-C\varphi\Delta/M. \tag{13}$$

Here, $M = R_{11}$, which is the magnification, and $C = R'_{12} = T_{126}$. When magnification M is greater than 1, image blurring is compressed by a factor of M, so chromatism is reduced. The chromatic factor can now be written as C/M [5].

Using the thin lens approximation, the chromatic factor can be written in a complicated form,

$$\begin{aligned}T_{126} = {} & (4D_1(D_2^2\ f_1^2+D_1^2(-2D_2^2+(f_1-f_2)^2) \\ & +D_1\ D_2(2f_1^2+f_2^2))+d(4D_1^2(-2D_2^2 \\ & +(f_1-f_2)^2)-2D_2\ f_1\ f_2^2+2D_1(3D_2^2\ f_1 \\ & +f_1(f_1-f_2)\ f_2+2D_2(f_1^2+f_2^2)))))/(f_1^2\ f_2^2),\end{aligned} \tag{14}$$

$$\begin{aligned}T_{346} = {} & (4D_1(D_2^2\ f_1^2+D_1^2(-2D_2^2+(f_1-f_2)^2) \\ & +D_1\ D_2(2f_1^2+f_2^2))+d(4D_1^2(-2D_2^2 \\ & +(f_1-f_2)^2)+2D_2\ f_1f_2^2+D_1(-6D_2^2\ f_1 \\ & +2f_1\ f_2(-f_1+f_2)+4D_2(f_1^2+f_2^2)))))/(f_1^2\ f_2^2).\end{aligned} \tag{15}$$

Numerical computations show that the two chromatic factors are not equal. With proper parameters, the chromatic factor of one direction can be much smaller than that of the $-I$ lens, but in the other direction the chromatic factor cannot be reduced significantly. We do not find a case where the two chromatic factors are both much smaller than those of the $-I$ lens.

Fourier planes of both the x-plane and y-plane exist. The two planes may not coincide for the magnifying lens. We will show that the two planes are very close in lengthened lens with the numerical simulation.

Since there is so much freedom, there are infinite configurations for a magnifying lens. A lengthened lens is only one of theses configurations. With the help of beam dynamics codes, we can get other configurations by searching the parameters of each element.

However, the lengthened lens has inherited many of the merits of the $-I$ lens. The structure is very simple and there are only two quadrupole excitation states. The approximate coincidence of the two Fourier planes is very useful for experiments.

4 An example of the magnifying lens design

In a lengthened lens, we see that parameter S should be close to parameter T to achieve magnification when the thin lens approximation is assumed. However, the expression is very complicated and hard to use. At the same time, real quadrupoles are not thin lenses, so beam dynamics codes are used to design the lens.

Nowadays, there are many beam dynamics codes. Here, the My-BOC code [6], which is based on Lie algebra, is used. The parameters can be confined in a specified interval when searched, since the BOBYQA algorithm developed by J.D. Powell is used [7]. This is very convenient when designing a beamline.

An example of the design is shown as Fig. 3, where the beam energy is 800 MeV, the highest gradient of quadrupoles is 11 T/m, and the length of the quadrupoles is 0.4 m.

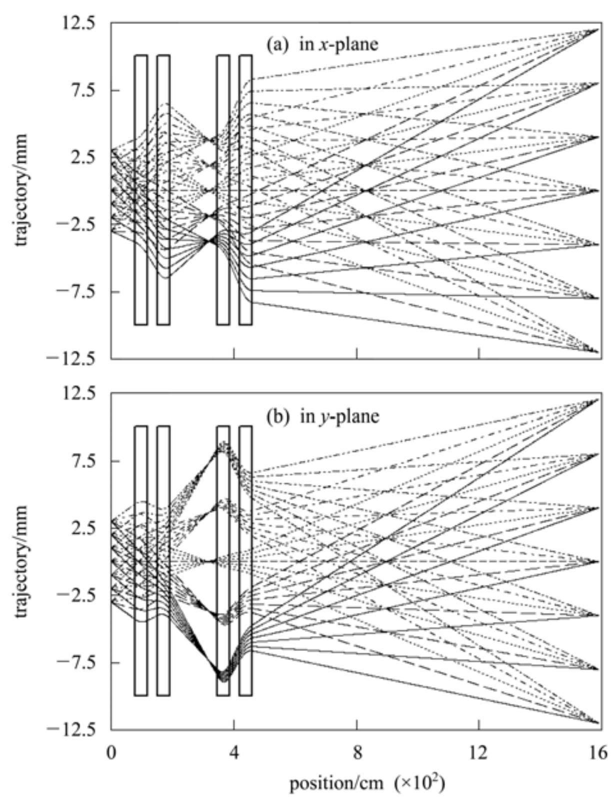

Fig. 3. Particle trajectories.

The magnification is −4 at both the x- and y-plane.

In this figure, we see that the two Fourier planes are very close. In fact they do not coincide. The distance between them is only a few millimeters. We changed the parameters of the lens, including the beam energy, the strength of the quadrupoles and the length of the drift spaces, and this status remained. We believe that this is true in all cases, but it is only now that we have got mathematical certification of this.

T_{126} is 18.94 and 36.13 m for the x- and y-plane of this lens individually. Unlike the $-I$ lens, the two factors are not equal. Consider Eq. (12), the chromatic factor is 4.74 and 9.03 m for the x- and y-plane individually.

A comparative design of an $-I$ lens with the same condition shows that the chromatic factor is 10.08 m for both the x- and y-plane. We can see that the chromatic factor reduces significantly in the x-plane, and reduces a little in the y-plane when using a magnifying lens.

Designs other than those using a lengthened lens were also studied, and many cases were acquired. For example, where the parameters of two or three quadrupoles and the lengths of some of the drift spaces varied freely. In some of these cases the image may be mirrored, that is $M_x = -M_y$, and many of them can also be used in proton radiography. However, in all the cases we studied, the distance between the two Fourier planes is large and the chromatic factors are similar to those of the lengthened lens.

5 Conclusion

In high-energy proton radiography, magnifying magnetic lenses may be used in microscopy systems. Based on the $-I$ lens proposed by Zumbro, we suggest a lens configuration called lengthened lens, which inherits the main merits of the Zumbro lens. Theoretical analysis shows that the lengthened lens can form a magnifying lens, and some relationships are given. Using the My-BOC beam dynamics code, an example design is shown, and the design results show that the method of designing magnifying magnetic lenses is effective.

References

1 King N S P, Ables E, Ken Adams et al. Nuclear Instruments and Methods in Physics Research A, 1999, **424**: 84–91

2 Hogan G E, Adams K J, Alrick K P et al. Proton radiography. Proceedings of the Particle Accelerator Conference, USA, New York: 1999, 579–583

3 Mottershead C Thomas, Zumbro John D. Magnetic Optics for Proton Radiography. Proceedings of the Particle Accelerator Conference. Canada Vancouvev: 1997. 1397–1399

4 HE Xiao-Zhong, YANG Guo-Jun, LIU Cheng-Jun. High Power Laser and Particle Beams, 2008, **20**(2): 297–300 (in Chinese)

5 Mottershead T, Barlow D, Bland B et al. Design and Operation of a Proton Microscope for Radiography at 800 MeV, Proceedings of the Particle Accelerator Conference. USA, Portland: 2003. 702–704

6 ZHANG Zhuo, YANG Guo-Jun, LÜ Jian-Qin. Chinese Physics C, 2010, **34**(1): 134–137

7 ZHANG Zhuo. Theoretic Analysis and Program Design for Nonlinear Transportation of Intense Beam. Thesis for Doctor' Degree. Beijing University, 2010